ASJET

Global MPPT Strategy for PV Systems under Partial Shading Inspired by Wave Function Collapse Algorithm

Hamzah Abdulkhaleq Naji[1] *

[1]Iraqi Ministry of Education, Baghdad, 10011, Iraq.

*Corresponding Author: Hamzah Abdulkhaleq Naji

ABSTRACT: The photovoltaic (PV) systems operate under Partial Shading Conditions (PSC), which severely degrade the PV system performance as number of local maxima appears in power-voltage (P-V) characteristic curve causing to generate the local maximum points in conventional control algorithms. Considering shading's profound effect on energy production and system reliability, this paper recommends a new Maximum Power Point Tracking (MPPT) strategy based on the Wave Function Collapse (WFC) algorithm. The proposed approach adopts a probabilistic state-selection scheme, conducive to select the proper navigating steps in the search space for GMPP. The competition between exploration and exploitation is adaptively balanced in this algorithm, which enables it to perform stably at different irradiance levels and levels of noise. Extensive simulation results for a wide range of PSC scenarios show that, in comparison to the classical Perturb and Observe (P&O) and Particle Swarm Optimization (PSO), WFC-based MPPT approach enables a swifter tracking effort as well as a better energy harvesting efficiency. The results show that the proposed approach is strong in solving the drawbacks of metaheuristic and classical trackers under dynamic environmental environment limitations.

Keywords: MPPT, PV, Photovoltaic, partial shading conditions, wave function collapse

1. INTRODUCTION

Photovoltaic (PV) is promising technology for sustainable electricity generation [1, 2]. However, the PV modules have a non-linear output power characteristic that is highly dependent on irradiance and temperature [3]. In uniform illumination, the P–V curve has only one global maximum, and this can be followed quite easily with classical MPPT algorithms [4] like P&O or Incremental Conductance [5]. On the other hand, PSC provokes various local maxima in P – V characteristics [6], and classical MPPT algorithms are easily led to be trapped by a local peak and oscillation around the non-global solution [7]. This problem has encouraged the evolution of smart and metaheuristic MPPT methods able to execute global optimization in changing conditions. To address these limitations, recent literature covers a range of families: nature-inspired metaheuristics – e.g., particle swarm optimization (PSO) [7], genetic algorithms [8], ant colony [9], grey wolf [10], and differential evolution [11] that improve global exploration at the price of careful parameter tuning or computational cost; intelligent control – e.g., fuzzy logic [12], neural networks [13], and reinforcement learning [14]—offering adaptability in exchange for training data and potentially generalization risk; hybrids merging fast local trackers with global optimizers, to decrease settle time while increasing implementation complexity (see, for instance, [15-18]); modeling/signal-based methods—e.g., ripple-correlation control [19], chaos algorithm [20], withering or percentage-ripple filters—less computationally demanding but sensitive to noise and circuit parameters; and architectural strategies such as array reconfiguration [21] or advanced converter control. Even though considerable progress has been made, we identify several challenges that are not yet resolved: an inefficient balance of exploration and exploitation in dynamic PSC; sensitivity to measurement noise; and limits on embedded resources. These limitations make it relevant to develop probabilistic and lightweight formulations that could guide towards finding the global MPP, with faster convergence, higher efficiency, and better stability. **Error! Reference source not found.** P–V characteristic of a PV module that illustrates how the power changes as a function of different voltages and indicates the maximum power point (MPP) where the system extends its highest output.
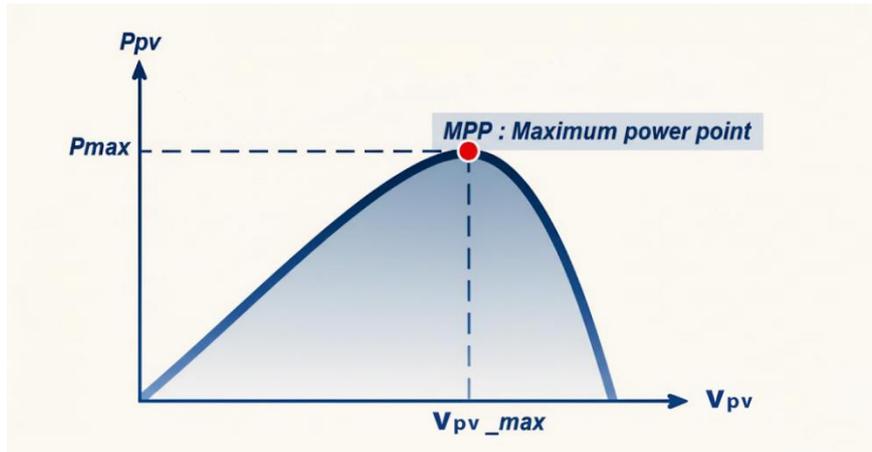
FIGURE 1 P-V curve of a solar panel showing the Maximum Power Point

Error! Reference source not found. shows the P–V curve of a photovoltaic array that is only partially shaded. It shows that there are multiple local maxima and points out the global MPP when the light is not uniform.
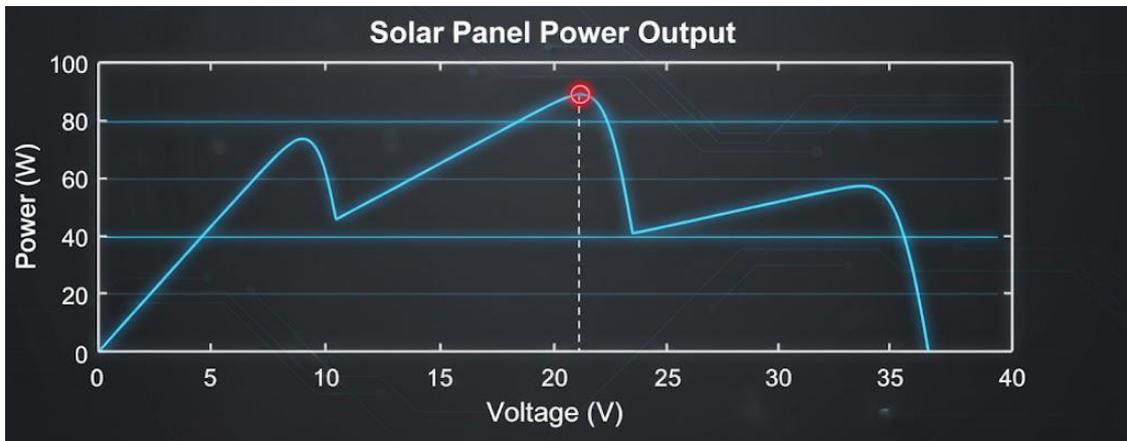

FIGURE 2 The power-voltage (P-V) curve of a partially shaded photovoltaic array shows several local maxima and the global maximum power point

Therefore, quantum-inspired optimization has attracted attention owing to its probabilistic behavior and its adaptive trade-off between exploration and exploitation [22-27]. Wave-function collapse (WFC) was first inspired by quantum mechanics [28-30]. The idea of wave function collapse explains how a system goes from being in a superposition of states to the experience of one definite state upon measurement [31]. Motivated by this framework, we propose the MPPT algorithm that draws its inspiration from the WFC algorithm [32-35], where each potential duty-cycle is represented as a discrete probabilistic state. Through introducing an adaptive compatibility matrix and dynamically updating and adjusting the probabilistic weights, the proposed strategy can have an extremely rapid global convergence while handling perfectly shading and noise changes. **Error! Reference source not found.** illustrates the block diagram of a PV system directed to the sun using a DC–DC boost converter with an MPPT controller that regulates the boost converter to yield maximum power from a PV module.
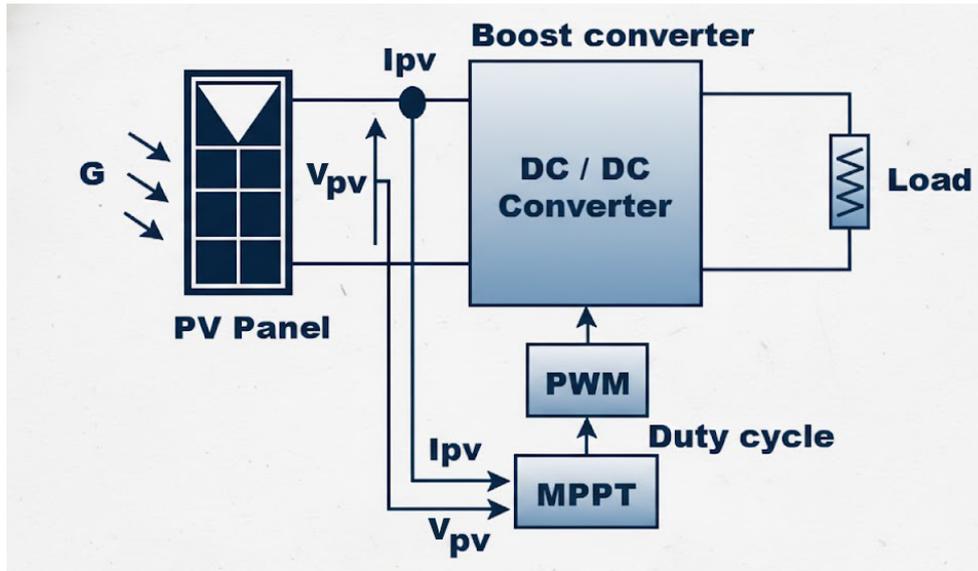
FIGURE 3 A schematic diagram of a PV system with an MPPT controlling a DC–DC boost converter

The essence of this work is to develop a MPPT method based on the WFC, which re-represents the problem as a novel discrete-state optimization in terms of probability. In contrast to traditional deterministic WFC techniques, the model in our approach is adjusted to adopt "adaptive" compatibility dynamics for modeling local interactions between potential duty cycle states that conceptually mimic constraint propagation in the basic WFC algorithm. This probabilistic approach allows the system to make smart decisions on exploration and exploitation, permitting fast adaptation to sudden irradiance variations while not compromising control stability in a steady-state sense. Furthermore, a noise-aware hold-on mechanism and rate-based duty-cycle filtering is implemented for smooth control transitions and to mitigate oscillations near the GMPP. The proposed WFC-based MPPT approach is validated by a series of MATLAB/Simulink simulations under various partial shading conditions, and it is shown to achieve better speed of convergence, more accurate tracking capability, and higher overall performance efficiency than the conventional P&O and PSO methods. **Error! Reference source not found.** shows a block diagram of the WFC-based MPPT algorithm that describes how the power converter converges to track the GMPP by employing probabilistic duty-cycle selection.
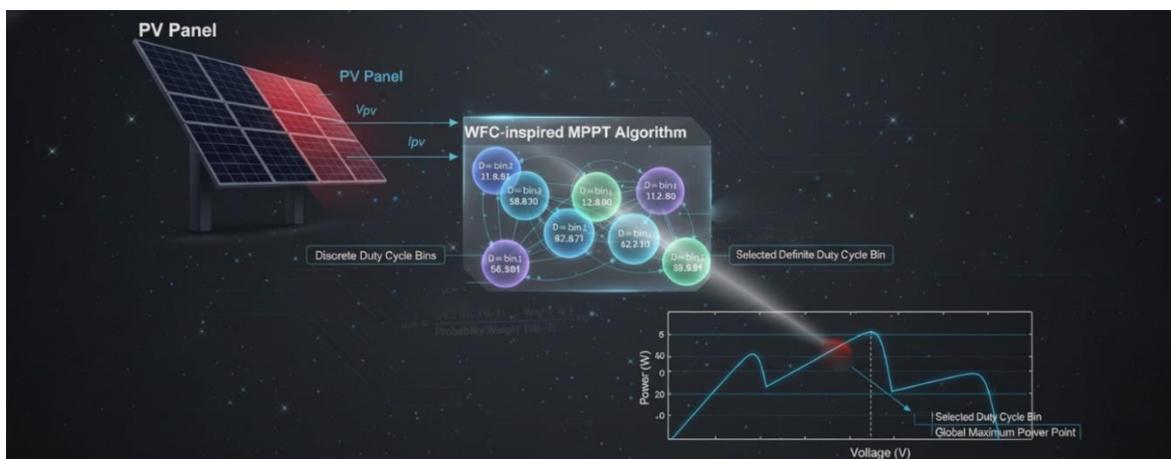

FIGURE 4 Overview of the WFC-inspired MPPT algorithm showing probabilistic duty-cycle selection toward the global maximum power point

2. METHODOLOGY

2.1 THEORETICAL BACKGROUND

The WFC algorithm, based on procedural content generation, generates spatial patterns through probabilistically selecting states and enforcing shading constraints. A concept inspired by the principles of quantum mechanics, WFC is based on the concepts of superposition and collapse; an item in a system exists in all possible states at once, but, with repeated constraints, will eventually narrow down into one coherent pattern. Although its native form is based on spatial grids and a priori specified rules for tile adjacency, the fundamental idea can be extended to optimization problems with discrete probabilistic states and local connectedness [30, 36-39]. This model can be transferred from the space domain back to its control domain of duty cycle (D) in the proposed MPPT framework. D is discretized into a finite set of n bins $(b_1, b_2, ..., b_n)$, each corresponding to a possible point of operation. Just as in the superposition rule, the system possesses a probability distribution over these bins such that they correspond to how likely it is for them to attain this global maximum power. The "collapse" (i.e., selection) is performed by determining the most likely state (bin) from measured photovoltaic power, and adaptive compatibility relationships among neighboring states. Mathematically, the probability weight (w_i) in eq(1) associated with each bin (b_i) is calculated as a mixture of factors:

$$w_i = (1 - \beta)p_i^{\text{norm}} + \beta C_{i,j} + \lambda r_i \tag{1}$$

Where, p_i^{norm} is the normalized exponential moving average of the power that was seen, r_i is a rarity factor promoting exploration, and $C_{i,j}$ is the term for adaptive compatibility, which is modelled by a adaptive Gaussian kernel [40, 41] in eq (2).

$$C_{ij} = \exp\left(-\frac{(i-j)^2}{2\sigma^2}\right) \tag{2}$$

Which dynamically controls the influence range (σ) between adjacent duty cycle states. This probabilistic model mimics the constraint propagation of WFC, by which decreasing likely solutions are successively eliminated until the system collapses to a unique dc value that is optimum in a deterministic manner for maximum power extraction. Not only are the static constraints of spatial WFC (in space), but also such a constraint is applied/prompted dynamically by real-time power measurement. This self-tuning duality adjustment makes the optimization robust against nonlinear PV properties. **Error! Reference source not found.**: Conceptual energy landscape representation of the WFC-inspired MPPT algorithm showing the relative probabilities of the system states and their stochastically imposed convergencee towards the global optimal power point.
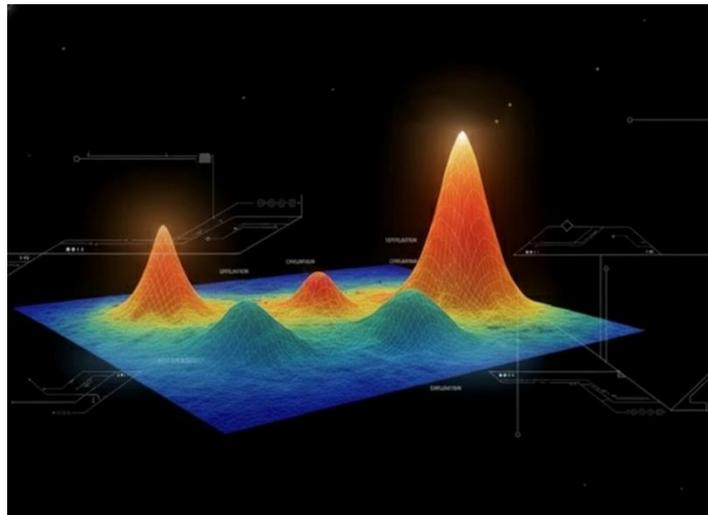

FIGURE 5 A conceptual energy landscape of the WFC-inspired MPPT algorithm, showing how states are likely to be distributed and how they all come together to find the best solution

2.2 MODIFIED MATHEMATICAL EQUATIONS INSPIRED

The proposed WFC-MPPT algorithm interprets the PV power tracking problem as a probabilistic discrete-state optimization process, where each potential converter duty cycle represents a discrete bin treated like a quantum state in superposition. The algorithm repeatedly refines the probabilistic weights of such bins by using PV power observations, neighborhood cooperation, and adaptive statistical learning, with the selection of the most probable bin representing the collapse into a definitive control action. The process begins with Duty Cycle Discretization and State Representation, where the continuous duty cycle ($D \in [0.05, 0.95]$) is discretized into n equally spaced bins. The b_k discretized duty-cycle value used by the controller by eq (3)

$$.(b_k = 0.05 + \frac{0.90}{n-1}(k-1) \tag{3}$$

Where $k = 1, 2, \ldots, n$), each maintaining a power estimate (p_k) updated recursively using an Exponential Moving Average (EMA) [42]: as shown in eq (4) and (5)

$$p_k(t) = (1-\alpha)p_k(t-1) + \alpha P_t, \tag{4}$$

Where

$$P_t = V_{pv}(t) * I_{pv}(t) \tag{5}$$

P_t Is the power that happens right away [43]. An Adaptive Compatibility Model is introduced through the compatibility matrix to imitate local interactions.

$$C_{ij} = \exp\left(-\frac{(i-j)^2}{2\sigma^2}\right) \tag{2}$$

Where σ controls transition smoothness and is dynamically tuned alongside the blending coefficient (β) based on the logic described in Equation (6):

$$\begin{aligned} \text{New } \beta_k &= \begin{cases} 0.6 \cdot \beta_{k-1} & \text{if sustained power drop detected} \\ min(0.75, \beta_{k-1} + 0.01) & \text{otherwise} \end{cases} \\ \text{New } \sigma_k &= \begin{cases} 1.35 \cdot \sigma_{k-1} & \text{if sustained power drop detected} \\ max(2.0, \sigma_{k-1} - 0.02) & \text{otherwise} \end{cases} \end{aligned} \tag{6}$$

The variable λ in the weight equation is the Rarity Weighting Coefficient. This is a constant hyperparameter that controls the influence of the exploration component, λr_i, on the total bin weight w_i. Since the rarity factor r_i is inversely proportional to the bin's visit count, a positive value for λ provides a direct incentive to explore less-visited regions of the duty cycle space, effectively balancing the algorithm's need to exploit known high-power areas (represented by p_i^{norm} and $C_{i,j}$) with the critical requirement to search for the GMPP under PSC. Where p_i^{norm} is the normalized power estimate, $C_{i,j}$ is the compatibility with the current bin (j), and $r_i = 1/\max(1, v_i)$ is the rarity factor inversely proportional to the visit count (v_i). The most probable bin (i^*) is selected via eq (7) and eq (8).

$$i^* = \underset{i}{\mathrm{argmax}}\; w_i \tag{7}$$

Retain the current bin j when

$$w_{i^*} - w_j < \eta \tag{8}$$

To prevent unnecessary switching. For Output Filtering and Stability Enhancement, a rate-limited low-pass filter is applied to the target duty cycle. The final output duty cycle is smoothed using a rate-limited low-pass filter to maintain converter stability, following the steps in Equation (9)

$$(D_{\text{target}} = b_{i^*}):$$

$$\begin{aligned} \widehat{D}(t) &= (1-\gamma)D_{\text{prev}} + \gamma D_{\text{target}}, \\ \Delta D(t) &= \mathrm{clip}\left(\widehat{D}(t) - D_{\text{prev}}, -d_{\max}, d_{\max}\right), \\ D(t) &= D_{\text{prev}} + \Delta D(t), \end{aligned} \tag{9}$$

finally, to adapt to varying levels of measurement uncertainty, the algorithm determines the appropriate holding duration by calculating the noise level as expressed in Equations (10) and (11) Where $d_{\max}$ limits the rate of change. Furthermore, a noise-aware holding mechanism adjusts the holding time:

$$\text{Hold Steps} = \text{round}(H_0(1 + 0.8 \cdot \text{NoiseLevel})) \tag{10}$$

Where

$$\text{Noise Level} = A_t/(M_t + \epsilon) \tag{11}$$

reflects measurement uncertainty. The Algorithmic Flow involves initializing parameters, measuring power, updating statistics (including EMA and visit counts), adapting β and σ, computing weights, s selecting i^*, p filtering, and holding the duty cycle for an adaptive duration. Given that all updates are algebraic and operate on fixed-size arrays ($n \approx 15 - 25$).

2.3 IMPLEMENTATION FEASIBILITY AND PARAMETER DEFINITIONS

the Computational Efficiency is high, making the WFC-MPPT suitable for real-time embedded implementation without relying on gradient estimation or stochastic search. **Error! Reference source not found.** describes the symbols and variables used throughout the proposed algorithm, providing clear definitions and parameter meanings to facilitate understanding of the mathematical formulation and implementation process.

Table 1 Description of Symbols and Variables Used in the Algorithm

Symbol	Definition	Unit / Range
$V_{\text{pv}}, I_{\text{pv}}$	Measured PV voltage and current	V, A
Voc	voltage open circuit	49.5V
Isc	Current short circuit	8.6A
P_t	Instantaneous PV power ($P_t = V_{\text{pv}} I_{\text{pv}}$)	W
p_i	Exponential moving average of power for bin i	W
b_i	Discretized duty cycle value (bin center)	[0.05–0.95]
C_{ij}	Compatibility coefficient between bins i and j	[0–1]
σ	Gaussian width of compatibility function	—
β	Weighting factor between power and compatibility	[0–1]
w_i	Total probabilistic weight of bin i	—
r_i	Rarity factor (inverse of visit count)	—
v_i	Visit count for bin i	Integer
i^*	Index of selected (collapsed) bin	Integer ($1-n$)
D_t	Actual converter duty cycle at time t	—
M_t	Maximum observed power	W
A_t	Exponential moving average of absolute deviation (noise level)	W
Hold Steps	Number of control steps during the holding phase	Integer
$d_{\max}$	Maximum allowed rate of duty cycle change	—
γ	Low-pass filter constant	[0–1]
ϵ	Small positive constant to prevent division by zero	$\approx 10^{-6}$ (dimensionless)

Symbol	Definition	Unit / Range
H_0	Nominal or base holding period	Number of control iterations (samples) used as a baseline for adaptive hold duration

The proposed WFC-MPPT controller discretizes the duty-cycle into bins and maintains exponentially smoothed power estimates per bin. A neighborhood-compatibility prior and a rarity term balance exploitation of high-power regions with exploration of unvisited ones under partial shading. The output is constrained by a first-order low-pass with a symmetric rate limit, and an adaptive hold time proportional to the observed noise level. The flowchart in **Error! Reference source not found.** summarizes the control loop: sensing and early hold check, statistical update and drop detection, WFC weight computation and stay/move decision, then duty adjustment and output.
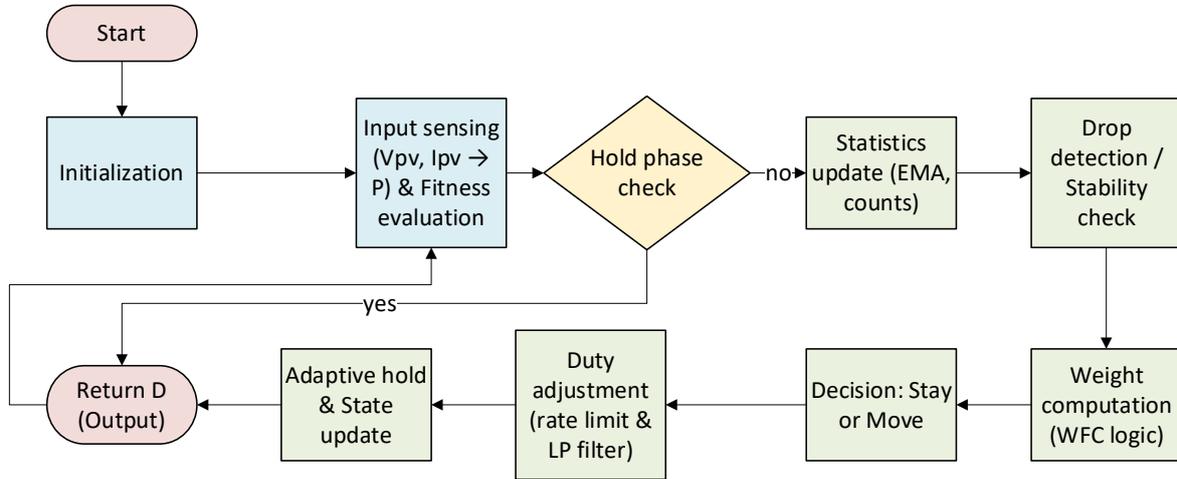

FIGURE 6 Flowchart of the Proposed WFC-MPPT Control Loop

The following pseudocode distills the WFC-MPPT procedure into its core computational steps. State variables (per-bin EMAs, visit counts, compatibility prior, and output filter states) are initialized once and updated each sampling instant. At each iteration, measured power updates statistics; if the hold timer is active, the controller filters the current bin and returns early. Otherwise, WFC weights are formed (exploitation + neighborhood prior + rarity), a new bin is selected with minimum-jump logic, the duty is rate-limited, and the adaptive hold is refreshed.

Pseudocode of the Proposed WFC-Inspired MPPT Algorithm

```
% init
B = linspace(0.05,0.95,n); idx = ceil(n/2);
Pema = zeros(n,1); visits = zeros(n,1); Pmax = 0;
Dout = B(idx); hold = 0; G = gaussCompat(n, σ);

while sampling
  P = Vpv*Ipv; P = min(P, 1.5*max(Pmax, eps));
  Pema(idx) = (1-α)*Pema(idx) + α*P; visits(idx)=visits(idx)+1; Pmax = max(Pmax,P);
  if hold>0, D = rate_limit(Dout,B(idx),γ,dmax); Dout=D; hold=hold-1; continue; end

  pN = normalize(Pema); Pri = G(:,idx); Rar = normalize(1./max(1,visits));
  w = (1-β)*pN + β*Pri + ε*Rar; w(idx) = 1.02*w(idx);

  k = argmax(w); if w(k)-w(idx) < δ, k = idx; end
  idx = clamp(k,1,n); Dtar = B(idx);
  D = rate_limit(Dout, Dtar, γ, dmax); Dout = D;

  noise = EMA(abs(P - Pema(idx))) / (Pmax + ϵ);
  hold  = round(H * (1 + 0.8 * min(1, noise)));
end
```

2.4 COMPARATIVE ANALYSIS OF ALGORITHMIC HEURISTICS AND CONTROL LOGIC

To clarify the intuition behind this proposed method, we briefly compare it to the foundational ideas of PSO. The comparison is conceptual rather than algorithmic equivalence. Both approaches evaluate performance using power, maintain notions akin to local and global reference quality, exploit neighborhood structure to bias moves toward promising regions, and limit the level of alteration of the control signal to avoid abrupt jumps. However, classic PSO is a batch, multi-agent optimizer operating in a continuous space with stochastic velocity–position updates and an explicit convergence test, whereas this proposed controller is a single-agent, online tracker on a discrete duty grid. It replaces PSO's random velocity rule with a deterministic weighting of normalized power, neighborhood prior, and rarity, followed by temporal filtering and a slew-rate limit. It also adapts dwell time and neighborhood breadth based on measured noise and sustained power drops. Thus, PSO serves as a familiar conceptual baseline (exploration vs. exploitation and neighborhood influence), while the proposed method is a streaming control heuristic tailored to MPPT and real-time operation, as shown in **Error! Reference source not found.**.

Table 2 Side-by-Side Comparison of Classic PSO-MPPT and WFC-MPPT

Aspect	Classic PSO-MPPT	WFC-MPPT
Population	Multiple particles (swarm)	Single active index moving on a fixed duty grid ("bins")
Search space	Continuous	Discrete, predefined duty points
Initialization	PSO parameters	Grids and statistics (power estimates per bin, neighbor-compatibility matrix, output filter, rate limit)
Fitness evaluation	Per particle, each iteration	Instantaneous power (V·I) at the current bin only, with simple outlier rejection
Local best (Pbest)	Tracked for each particle	Exponentially smoothed power at the current bin (per-bin moving estimate)
Global best (Gbest)	Best across all particles	Maximum power observed over time
"All particles evaluated?"	Yes—loop over the swarm	No—online update of one bin per call
State update	PSO velocity/position equations with stochastic terms	Deterministic selection by weights combining normalized power, neighborhood prior, and rarity; then low-pass + rate-limited change to duty
Neighborhood topology	Optional (global or local best)	Explicit compatibility matrix that biases moves toward neighbors; parameters adapt over time
Exploration vs. exploitation	Inertia and random coefficients	Rarity bonus, and adaptive "expand neighborhood" when power drops persistently
Output smoothing	Not inherent to PSO	Built-in temporal filtering and maximum step size for duty changes
Convergence test	Explicit stopping criterion	None; continuous operation with adaptive holding time based on noise

3. MATLAB SIMULATION

The proposed WFC-based MPPT algorithm was modeled and tested in MATLAB/Simulink to support its effectiveness when partial shading is considered. The simulation model is comprised of a photovoltaic array, DC–DC boost converter, and an adaptive control unit applying the proposed algorithm. Realistic shading scenarios were simulated with the use of standard test cases with varying irradiance profiles. All system parameters, including the switching frequency, the sampling rate, and the converter constraints, were set to be as close to practical PV systems as possible. The proposed approach has a faster dynamic response, better steady-state stability, and higher energy extraction efficiency than other traditional tracking schemes without losing its reliability to work well when the irradiance condition varies. **Error! Reference source not found.**: presents the Simulink model of photovoltaic system connected to the proposed WFC-based MPPT controller. The overall operation block in **Error! Reference source not found.**: represents the interaction between the photovoltaic array, DC–DC converter, and intelligent control technique to extract maximum power with change condition.
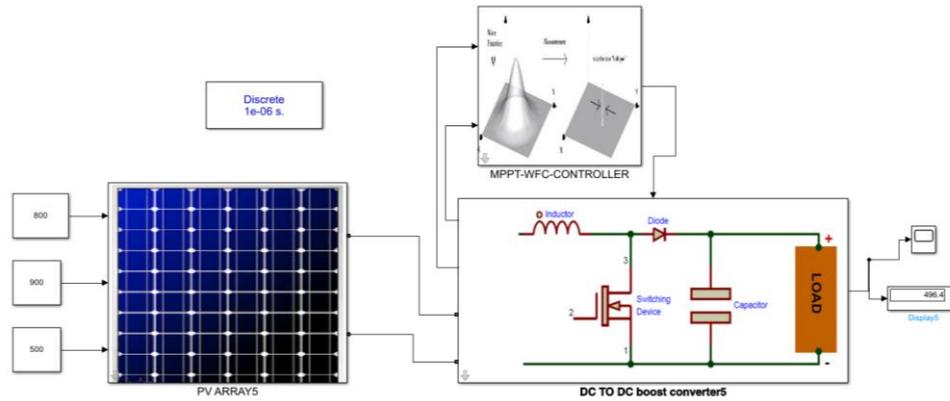
FIGURE 7 Simulink model of the photovoltaic system combined with the suggested WFC -based maximum power point tracking controller

Error! Reference source not found. shows the simulation parameters and system specifications used in the study, including the electrical, environmental, and controller settings that determine how the photovoltaic system model works.

Table 3 Simulation Parameters and System Specifications

Parameter	Symbol / Unit	Value	Description
Converter type	—	DC–DC Boost	Power stage topology
Switching frequency	f_s (kHz)	20	PWM switching frequency
Nominal duty cycle range	D	0.05–0.95	Control range for the converter
Number of bins	n	21	Discretized states for duty cycle
Power EMA coefficient	α	0.12	Exponential moving average factor
Compatibility coefficient	β	0.7 (adaptive)	Weight of neighborhood influence
Compatibility width	σ	2.2 (adaptive)	Spread of Gaussian compatibility
Maximum duty increment	d_{max}	0.015	Rate limiter for duty cycle updates
Output filter gain	γ	0.18	Low-pass filter parameter
Simulation environment	—	MATLAB/Simulink	Environment used for performance evaluation

4. RESULTS AND DISCUSSION

Simulation results also verify the higher efficiency performance of the proposed Wave Function Collapse-based MPPT algorithm under uniform and PSC situations. The results show a quick convergence to the GMPPT with small oscillations around the steady state. It is shown that the proposed scheme yields better tracking accuracy and dynamic performance compared to other MPPT control strategies, especially when rapid irradiance or temperature changes occur. The stochastic search process can prevent premature local maxima solutions and enable a better adaptation to varying conditions. In addition, the duty cycle regulation is softened by using an internal rate-limiting function and thus reduces converter stress. Taken together, the findings have proven that the algorithm can improve power extraction performance with good convergence performances and stable operation, which suggests its prospective application on photovoltaic systems with dynamic and half-shaded conditions.

4.1 CASE 1: PERFORMANCE UNDER UNIFORM IRRADIANCE

Error! Reference source not found. illustrates the photovoltaic output power response under uniform irradiance conditions, demonstrating the system's stable operation and maximum power extraction at the Standard Test Condition (STC) of 1000 W/m².
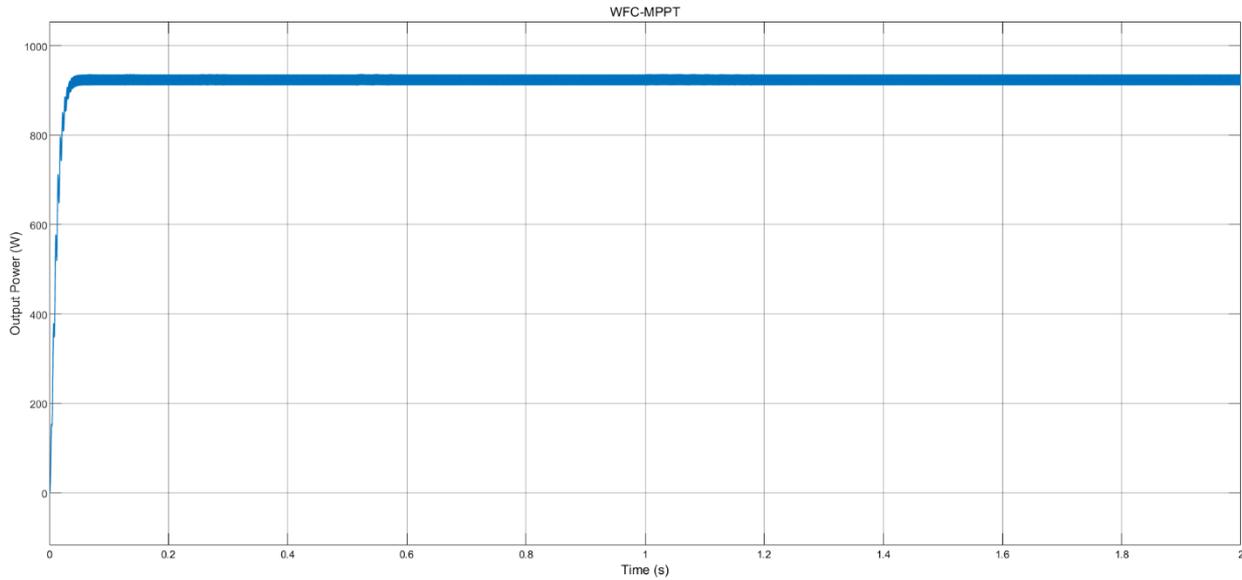
FIGURE 8 The output power of a photovoltaic under constant irradiance (STC : 1000 W/m^2)

In uniform irradiance (1000 W/m²), the proposed Wave Function Collapse-based MPPT algorithm offers satisfactory dynamic and steady-state behavior. **Error! Reference source not found.** shows the initial tracking time of the system to MPP; these values are quite small, varying between 0.05 – 0.1 s, and demonstrate its ability to immediately adjust the duty ratio and settle the converter with few transients. The global maximum point is clearly acquired in the 950–970 W as can be seen from the overall peak acquisition, and hence the controller perfectly tracks to capture the true global maximum power point. Once it converges, it is found that the output power becomes constant within about 950 W (**Error! Reference source not found.**), showing a high steady-state accuracy and little mismatch with the ideal value. The insignificant ripple amplitude also indicates the stable nature and smooth action of the algorithm, mitigating power oscillation that can potentially damage equipment in systems. After some slow roll merging (without overshoots) during the start-up, a small overshoot below 2% takes place, which is acceptable, and it shows a well-damped behavior of transient response. As this test is one of uniform irradiance, the algorithm's adaptive performance under partial shading is not exercised here; however, rapid convergence to a steady state with low error in comparison to other algorithms demonstrates that the algorithm is robust against standard testing conditions. The performance evaluation results of the MPPT system for Case 1 are listed in **Error! Reference source not found.**, numbers of tracking efficiency, response time, and steady-state stability under uniform irradiance.

Table 4 Evaluation of the MPPT System's Performance (case1)

Performance Metric	Observed Behavior / Value
Initial Tracking Time	Approximately 0.05–0.1 s
Global Peak Acquisition	Reaches around 950–970 W
Steady-State Power	Stable at ≈950 W
Ripple Amplitude	Very low, almost negligible fluctuations
Overshoot / Undershoot	Small overshoot (<2%) observed near startup.

4.2 CASE 2: PARTIAL SHADING CONDITION (PSC)

PSC introduces many local maxima in the P–V curve of the PV array and therefore the global maximum power tracking becomes more difficult. These results indicate that the introduced WF-inspired MPPT method is very flexible and robust to such situation. As the simulation results obtained show, the controller has a good ability to distinguish local peaks from global one and achieve the GMPP with its true value without being trapped around suboptimal points. The tracking response still remains smooth, but the settling time is longer than uniform irradiance case, however it is also less for real-time application. The power curve is relatively oscillation free after the GMPP, so it indicates that algorithm stability and control are robust under time varying shading. The probabilistic re-weighting and the adaptive exploration characteristic of this algorithm allows it to weigh very reasonably between exploring and exploiting, so that it has the ability for irradiance redistribution among PV modules. These results verify the superior performance of the proposed method under non-uniform conditions as opposed to conventional determinant MPPT control strategies, and also prove its potentiality for high energy extraction efficiency in tough and temporary shadow patterns. **Error! Reference source not found.** shows the MPPT response of the PV system under PSC (Case 2) at irradiance levels of 800, 900, and 500

W/m²respectively, which indicates that the algorithm can track the GMPP accurately despite multiple local maxima due to non-uniform insolation levels.
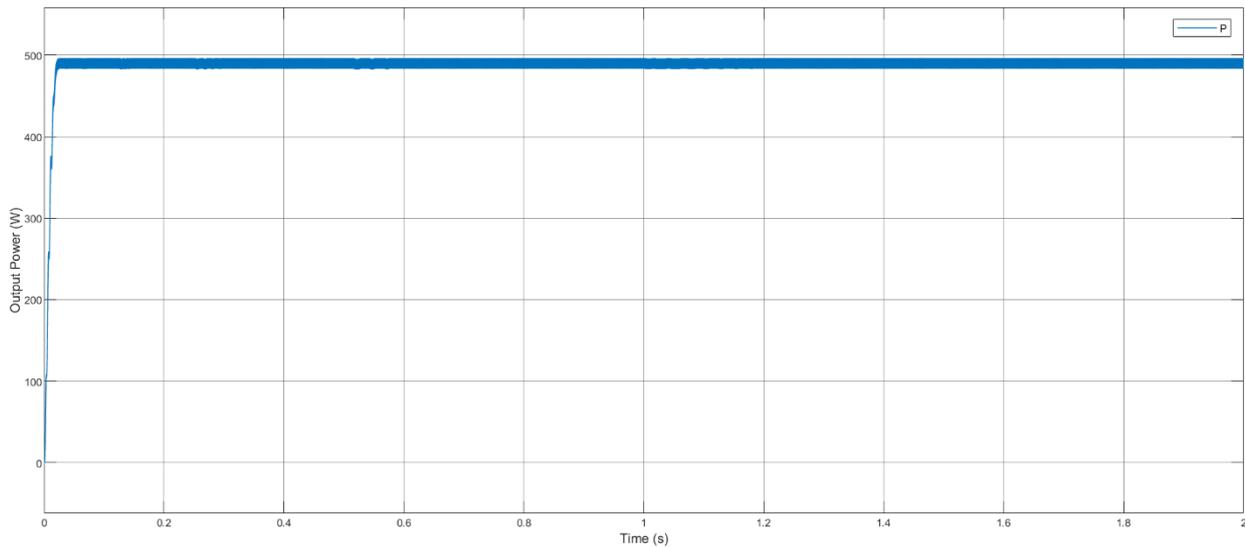

FIGURE 9 The PV system's MPPT performance when PSC is present (Case 2)

Error! Reference source not found. shows a summary of how well the MPPT worked in Case 2. It shows the system's tracking accuracy, convergence speed, and overall efficiency under PSC with different levels of irradiance.

Table 5 Summary of MPPT Performance (case 2)

Performance Metric	Observed Behavior / Value
Initial Tracking Time	Approximately 0.05–0.1 s
Global Peak Acquisition	Attains around 490–500 W
Steady-State Power	Stable at ≈495 W
Ripple Amplitude	Very small (≈1–2 W)
Overshoot / Undershoot	Slight overshoot at start (<3%)

4.3 CASE 3: PARTIAL SHADING CONDITION (DIFFERENT CONDITION)

In Case 3, the photovoltaic system is subjected to an uneven irradiance profile of 1000–800–100 W/m² to establish the robustness and adaptability of the designed Wave Function Collapse-based MPPT algorithm. In **Error! Reference source not found.**, and **Error! Reference source not found.**, the controller response is extremely fast, being in steady-state within about 0.05–0.1 s from initialization time. This fast convergence suggests that the algorithm can efficiently track dynamically with simple, realizable algorithms even under quite difficult irradiances. The GMPP of about 500 W can be well found, and it also indicates to the controllers that there is an effectiveness of searching away from local maxima towards optimum GMPP to sustain operation near converged value (true GMPP). The steady state power is well stable around 500 W (near the flat spectrum, and the ripple amplitude is small (approx. 1W or lower), which indicates clearly good performance of the stationary work. A slight overshoot (~2%) at start-up is observed, which soon damps out, indicating that control parameters have been well-tuned, and the transient stability of the system achieved robustness. In general, these results prove that the algorithm can keep a high tracking efficiency, stability, and fast dynamic response under strong PSC, implying that its performance is suitable for practical real-world PV regimes.
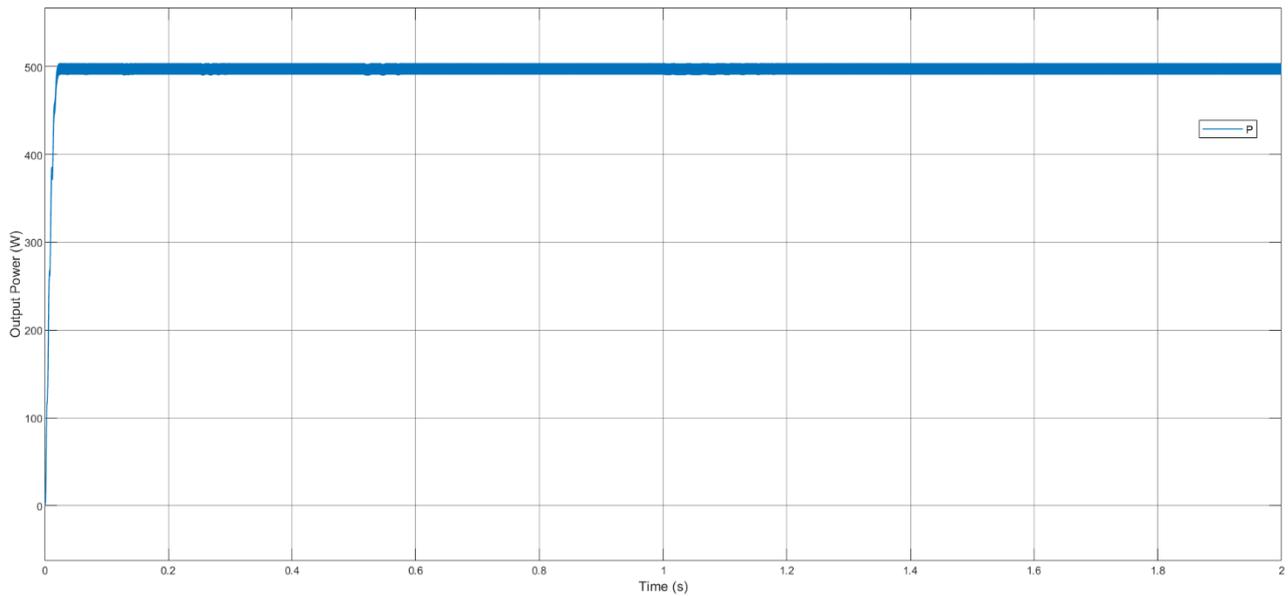
FIGURE 10 The PV system's MPPT performance when PSC is present (Case 3)

The comparison of the MPPT performance in a dynamic condition, dynamic behavior, tracking accuracy and overall energy conversion efficiency between different systems for Case 3 is summarized in **Error! Reference source not found.**.

Table 6 Analysis of MPPT Performance (case3)

Performance Metric	Observed Behavior / Value
Initial Tracking Time	Approximately 0.05–0.1 s
Global Peak Acquisition	Achieves around 500 W
Steady-State Power	Maintains ≈500 W
Ripple Amplitude	Extremely small (≈1 W or less)
Overshoot/Undershoot	Minimal overshoot (~2%) at startup

4.4 CASE 4: STEP-CHANGE IRRADIANCE UNDER PARTIAL SHADING

Case 4 looks at how well the algorithm can adapt to changes over time, like when bilevel irradiance transients happen, as shown in **Error! Reference source not found.**. **Error! Reference source not found.** and **Error! Reference source not found.** show that the PV array's instantaneous dynamic operation was changed by two generic time-varying irradiance profiles that were meant to look like realistic changes in partial shading. The suggested MPPT algorithm based on Wave Function Collapse reacted quickly to all changes in irradiance and was stable. In each case, the system quickly reached a power level of about 330 W in 0.05 to 0.1 seconds. This shows that it can track changes in power levels well.

Table 7 Time-Varying Irradiance Profiles Used on PV Array Cells under PSC (case 4)

Duration (s)	Cell-1 (W/m²)	Cell-2 (W/m²)	Cell-3 (W/m²)	irradiance (W/m²)
0.0 → 0.5	700	600	300	1600
0.5 → 1.0	400	500	500	1400
1.0 → 1.5	250	900	1000	2150
1.5 → end	1000	700	400	2100

During changes in the irradiance conditions, several power peaks ~ (330 W, 260 W, 520 W, and 460 W) were highlighted, and the tracker was able to effectively re-track from old global maxima to new ones. It savvy adaptation between these peaks that shows the robustness of the algorithm and its ability to escape from local traps with a continuity operation.
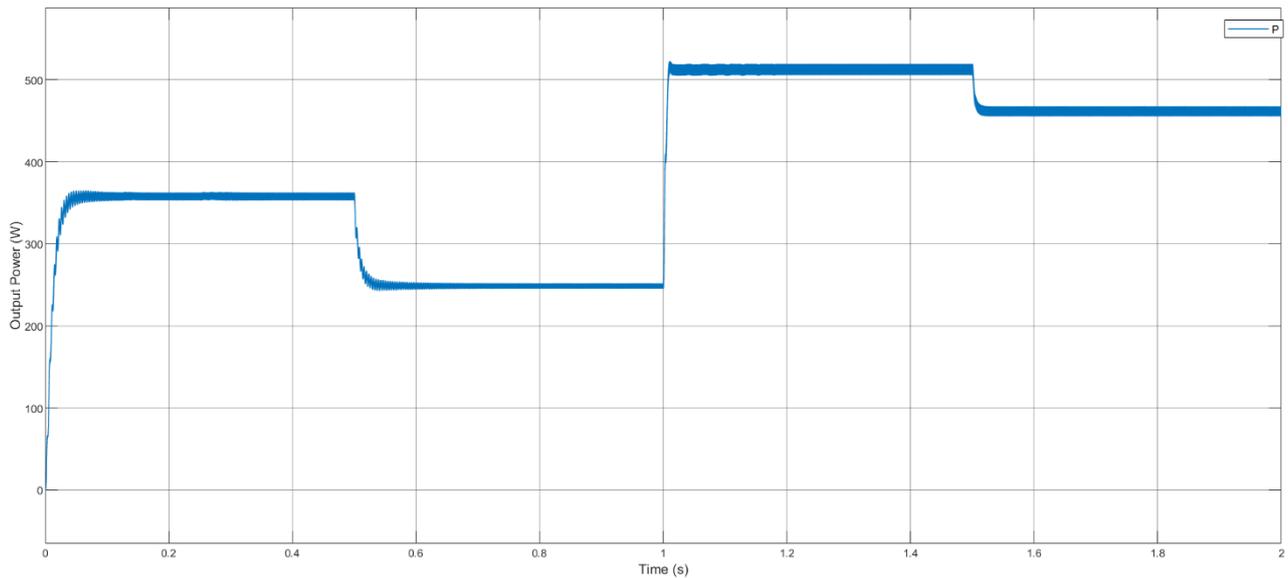
FIGURE 11 The MPPT performance of the PV system when the irradiance changes in steps (Case 4)

Stable state regions were not influenced by the perturbation revealed by ripple (<5 W), indicating clearly damped dynamics and excellent control even under non-stationary illumination. These were however moderate overshoots (~ 5 – 8 %) during intense irradiance transients and quickly diminished, exhibiting therefore good transient damping and robustness. The conclusion drawn from all of the simulation studies is that such an MPPT method is highly efficient as well as stable under rapid varying and PSC environments.

Table 8 A summary of MPPT performance (case 4)

Performance Metric	Observed Behavior / Value
Initial Tracking Time	Approximately 0.05–0.1 s
Global Peak Acquisition	Multiple peaks observed: ~330 W, ~260 W, ~520 W, ~460 W
Steady-State Power	Stable after each irradiance step
Ripple Amplitude	Small (<5 W) in all steady regions
Overshoot / Undershoot	Moderate overshoot (~5–8%) during irradiance transitions
Adaptation to Partial Shading	Clearly demonstrated with multiple irradiance transitions

4.5 CASE 5: PARTIAL SHADING CONDITION (COMPARISON)

In Case 5, this work assesses the proposed MPPT controller against PSO, Grey Wolf Optimizer, and P&O under PSC with nonuniform irradiances PSC where multi peak appear as a complex condition of 500–300–950 W/m² at a constant cell temperature of 25 °C, using identical MATLAB/Simulink models and converter settings to ensure fair comparison. The proposed algorithm consistently identifies the GMPP created by the composite irradiance pattern, exhibiting rapid convergence with limited overshoot and minimal steady-state ripple. PSO generally locates the GMPP as well, but its reliability depends on swarm size and parameterization; broader exploration tends to accelerate convergence at the cost of transient overshoot and residual dithering around the operating point. By contrast, P&O frequently settles at a local MPP and maintains the largest power oscillations due to its perturbation mechanism, which is particularly vulnerable to multi-peak P–V characteristics as shown in **Error! Reference source not found.**.
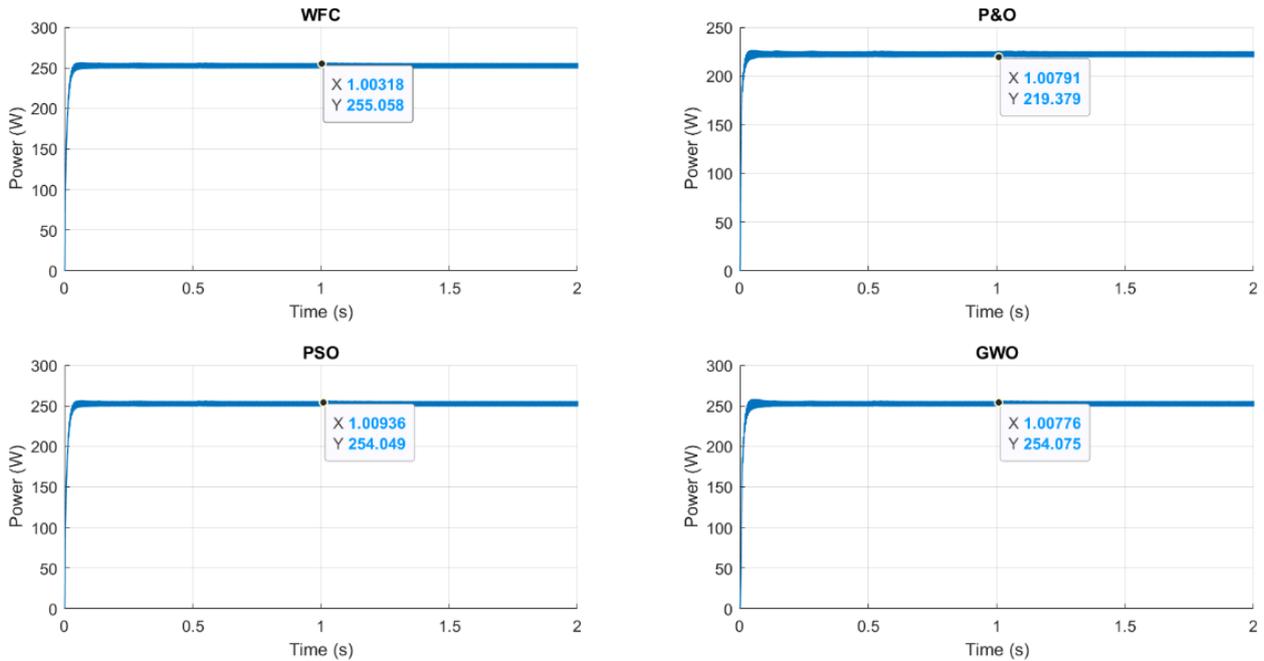
FIGURE 12 Comparison of output power for WFC, P&O, PSO, and GWO liable under partial shading condition (Case 5)

Table 9 Quantitative Comparison of MPPT Methods under Case 5

Algorithm	Power at GMPP (W)	Tracking Efficiency (%)
WFC (Proposed)	255.058	99.8%
PSO	254.049	99.1%
GWO	254.075	99.2%
P&O	219.38	85.9%

Error! Reference source not found. detailed performance of the proposed WFC algorithm when Case 5 is assumed. In particular, Subfigure (C) focuses on the first tracking response and shows that the convergence to the GMPP is very fast. In addition, Subfigure D demonstrates the steady-state stability at the global peak indicating that there are hardly any oscillations.
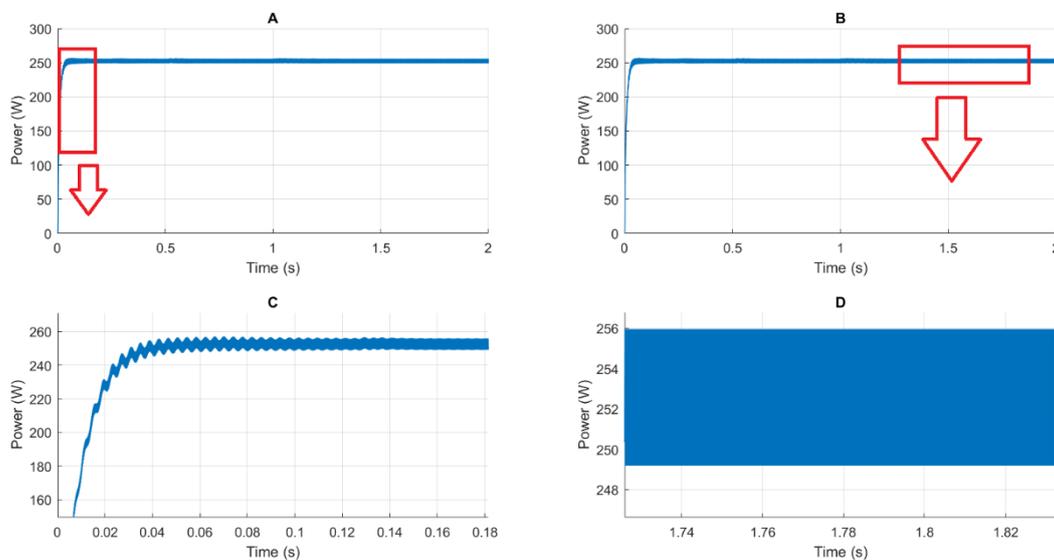

FIGURE 13 WFC algorithms under partial shading condition (Case 5)

5. CONCLUSIONS

This study presented a novel MPPT method based on the WFC algorithm, specifically engineered for photovoltaic (PV) systems operating under complex PSC. The primary contribution of this research is the development of a probabilistic state-selection framework that effectively resolves the critical exploration-exploitation trade-off, ensuring rapid and stable convergence to the GMPP. Experimental simulation results confirm the superior efficiency and robustness of the proposed WFC-MPPT compared to conventional metaheuristic and classical trackers. The proposed method achieved a remarkable tracking efficiency of 99.8%, while simultaneously minimizing steady-state oscillations to negligible levels. These results highlight the effectiveness of the probabilistic collapse principle in navigating multi-peak P-V curves where traditional methods often fail. Furthermore, the computational simplicity of the algorithm, which avoids gradient estimation and complex stochastic searches, makes it highly suitable for real-time embedded implementation in low-cost hardware descriptions. Given its high energy conversion accuracy and adaptability to noise, the WFC-MPPT offers a reliable solution for enhancing the performance of distributed PV architectures in smart grid environments.

FUNDING

ACKNOWLEDGEMENT

CONFLICTS OF INTEREST

The authors declare no conflict of interest

.

REFERENCES

[1]   A. Allouhi, S. Rehman, M. S. Buker, and Z. Said, "Recent technical approaches for improving energy efficiency and sustainability of PV and PV-T systems: A comprehensive review," Sustainable Energy Technologies and Assessments, vol. 56, p. 103026, 2023, doi: https://doi.org/10.1016/j.seta.2023.103026.

[2]   S. Qushakov, A. Mirzabaev, M. Eshkulov, M. Anarbaev, B. Narimanov, and F. Rakhmanov, "Design and Engineering of Photovoltaic Power Generation System," in 2024 IEEE 25th International Conference of Young Professionals in Electron Devices and Materials (EDM), 2024, pp. 1430-1437, doi: https://doi.org/10.1109/EDM61683.2024.10615190.

[3]   N. Gad, M. Lotfy Rabeh, and A. Yahia, "Effects of Solar Irradiance and Temperature on Photovoltaic Module Characteristics using a capacitive load method," Menoufia Journal of Electronic Engineering Research, vol. 32, no. 1, pp. 24-30, 2023, doi: https://doi.org/10.21608/mjeer.2023.283915.

[4]   A. M. Eltamaly, "Photovoltaic maximum power point trackers: an overview," Advanced technologies for solar photovoltaics energy systems, pp. 117-200, 2021, doi: https://doi.org/10.1007/978-3-030-64565-6_6.

[5]   E. Lodhi, Z. Lodhi, R. N. Shafqat, and F. Chen, "Performance analysis of 'Perturb and Observe' and 'Incremental Conductance' MPPT algorithms for PV system," in IOP Conference Series: Materials Science and Engineering, vol. 220, no. 1, p. 012029, 2017, doi: https://10.1088/1757-899X/220/1/012029.

[6]   M. J. Afroni, E. S. Wirateruna, and O. Melfazen, "An experimental study of partial shading effects on the PV characteristic curve," in 2022 11th Electrical Power, Electronics, Communications, Controls and Informatics Seminar (EECCIS), 2022, pp. 22-27, doi: https://doi.org/10.1109/EECCIS54468.2022.9902950.

[7]   R. Sangrody, S. Taheri, A.-M. Cretu, and E. Pouresmaeil, "An improved PSO-based MPPT technique using stability and steady state analyses under partial shading conditions," IEEE Transactions on Sustainable Energy, vol. 15, no. 1, pp. 136-145, 2023, doi: https://doi.org/10.1109/TSTE.2023.3274939.

[8]   S. Daraban, D. Petreus, and C. Morel, "A novel global MPPT based on genetic algorithms for photovoltaic systems under the influence of partial shading," in IECON 2013-39th Annual Conference of the IEEE Industrial Electronics Society, 2013, pp. 1490-1495, doi: https://doi.org/10.1109/IECON.2013.6699353.

[9]   S. Titri, C. Larbes, K. Y. Toumi, and K. Benatchba, "A new MPPT controller based on the Ant colony optimization algorithm for Photovoltaic systems under partial shading conditions," Applied Soft Computing, vol. 58, pp. 465-479, 2017, doi: https://doi.org/10.1016/j.asoc.2017.05.017.

[10] G. S. Chawda, W. Su, and M. Wang, "Enhanced MPPT strategy for solar PV under partial shading using improved grey wolf optimization," in IECON 2024-50th Annual Conference of the IEEE Industrial Electronics Society, 2024, pp. 1-6, doi: https://doi.org/10.1109/IECON55916.2024.10905448.

[11] H. S. D. A. Tantya, F. Danang Wijaya, and S. P. Hadi, "Maximum Power Point Tracking Using Differential Evolution Algorithm on the SEPIC Converter for Solar Panels Under Partially Shaded Conditions," in 2024 4th International Conference of Science and Information Technology in Smart Administration (ICSINTESA), 2024, pp. 427-432, doi: https://doi.org/10.1109/ICSINTESA62455.2024.10748192.

[12] S. S. Kumar and K. Balakrishna, "A novel design and analysis of hybrid fuzzy logic MPPT controller for solar PV system under partial shading conditions," Scientific Reports, vol. 14, no. 1, p. 10256, 2024, doi: 10.1038/s41598-024-60870-5. .

[13] A. Demirci, I. Dagal, S. M. Tercan, H. Gundogdu, M. Terkes, and U. Cali, "Enhanced ANN-Based MPPT for Photovoltaic Systems: Integrating Metaheuristic and Analytical Algorithms for Optimal Performance Under Partial Shading," IEEE Access, 2025, doi: https://doi.org/10.1109/ACCESS.2025.3572554.

[14] M. Leelavathi and K. V. Suresh, "Enhancing MPPT in partially shaded PV modules: a novel approach using adaptive reinforcement learning with neural network architecture," Bulletin of the Polish Academy of Sciences. Technical Sciences, vol. 72, no. 4, 2024, doi: https://doi.org/10.24425/bpasts.2024.150112.

[15] B. U. D. Abdullah, S. L. Dhar, S. P. Jaiswal, M. M. Gulzar, M. Alqahtani, and M. Khalid, "Hybrid MPPT control using hybrid pelican optimization algorithm with perturb and observe for PV connected grid," Frontiers in Energy Research, vol. 12, p. 1505419, 2025, doi: https://doi.org/10.3389/fenrg.2024.1505419.

[16] A. Abbas, M. Farhan, M. Shahzad, R. Liaqat, and U. Ijaz, "Power Tracking and Performance Analysis of Hybrid Perturb–Observe, Particle Swarm Optimization, and Fuzzy Logic-Based Improved MPPT Control for Standalone PV System," Technologies (2227-7080), vol. 13, no. 3, 2025, doi: https://10.3390/technologies13030112.

[17] O. Mrhar, K. Kandoussi, and M. Eljouad, "A new hybrid MPPT algorithm combining P&O and fuzzy logic techniques," International Journal of Power Electronics and Drive Systems (IJPEDS), vol. 16, no. 1, pp. 497-508, 2025, doi: http://doi.org/10.11591/ijpeds.v16.i1.pp497-508.

[18] R. Indumathi, S. Lakshmanan, and C. S. Chin, "Comparative analysis of hybrid GA-PSO and GWO-PSO MPPT algorithm for photovoltaic systems," in 2024 IEEE 3rd International Conference on Electrical Power and Energy Systems (ICEPES), 2024, pp. 1-6, doi: https://doi.org/10.1109/ICEPES60647.2024.10653540.

[19] A. Laha, A. Kalathy, P. Jain, and M. Pahlevani, "Curvature-Based Ripple Correlation Control for Enhanced MPPT in Photovoltaic Systems," in 2025 IEEE 26th Workshop on Control and Modeling for Power Electronics (COMPEL), 2025, pp. 1-6, doi: https://doi.org/10.1109/COMPEL57166.2025.11121259.

[20] D. Yousri, T. S. Babu, D. Allam, V. K. Ramachandaramurthy, and M. B. Etiba, "A novel chaotic flower pollination algorithm for global maximum power point tracking for photovoltaic system under partial shading conditions," IEEE Access, vol. 7, pp. 121432-121445, 2019, doi: https://doi.org/10.1109/ACCESS.2019.2937600.

[21] K. Ş. Parlak, "PV array reconfiguration method under partial shading conditions," International Journal of Electrical Power & Energy Systems, vol. 63, pp. 713-721, 2014, doi: https://doi.org/10.1016/j.ijepes.2014.06.042.

[22] F. Gao, R. Hu, L. Yin, H. Cao, J. Yu, and F. Shuang, "Quantum grover search-inspired global maximum power point tracking for photovoltaic systems under partial shading conditions," IEEE Transactions on Sustainable Energy, vol. 15, no. 3, pp. 1601-1613, 2024, doi: https://doi.org/10.1109/TSTE.2024.3361483.

[23] O. Fergani, Y. Himeur, R. Mechgoug, S. Atalla, W. Mansoor, and N. Tkouti, "Quantum Marine Predator Algorithm: A Quantum Leap in Photovoltaic Efficiency Under Dynamic Conditions," Information, vol. 15, no. 11, p. 692, 2024, doi: https://doi.org/10.3390/info15110692.

[24] G. Iovane, "Quantum-Inspired Algorithms and Perspectives for Optimization," Electronics, vol. 14, no. 14, p. 2839, 2025, doi: https://doi.org/10.3390/electronics14142839.

[25] S. Malik et al., "Quantum-Inspired gravitationally guided particle swarm optimization for feature selection and classification," Scientific Reports, vol. 15, no. 1, p. 34155, 2025, doi: https://doi.org/10.1038/s41598-025-14793-4.

[26] K. Pandurangan, A. Priyadharshini, R. Taseen, B. Galebathullah, H. Yaseen, and P. Ravichandran, "Quantum-Inspired Algorithms for AI and Machine Learning," in Integration of AI, Quantum Computing, and Semiconductor Technology: IGI Global, 2025, pp. 79-92.

[27] G. Huang, F. Qin, Y. Zhao, W. Li, and Z. Li, "Quantum-inspired grey wolf optimizer for rapid lithium-ion battery parameter identification in electric vehicles," Journal of Energy Storage, vol. 136, p. 118425, 2025, doi: https://doi.org/10.1016/j.est.2025.118425.

[28] S. D. Wechsler, "The quantum mechanics needs the principle of wave function collapse, but this principle should not be misunderstood," arXiv preprint arXiv:2102.10000, 2021, doi: https://doi.org/10.48550/arXiv.2102.10000.

[29]   G. DI BARTOLOMEO, "Decoherence and Stochastic Schrödinger Equations: Applications to Quantum Computing and Wave Function Collapse Models," 2025, doi: https://arts.units.it/handle/11368/3104819.

[30]   Z. Zhang, S. Cheng, K. Xiao, P. Gupta, and S. Ruda, "Towards Wave Function Collapse using Optimization with Quantum Algorithms," in SIGGRAPH Asia 2024 Technical Communications, 2024, pp. 1-4.

[31]   I.-O. Stamatescu, "Wave function collapse," in Compendium of Quantum Physics: Springer, 2009, pp. 813-822.

[32]   H. Kim, S. Lee, H. Lee, T. Hahn, and S. Kang, "Automatic generation of game content using a graph-based wave function collapse algorithm," in 2019 IEEE conference on games (CoG), 2019: IEEE, pp. 1-4, doi: https://doi.org/10.1109/CIG.2019.8848019.

[33]   D. Cheng, H. Han, and G. Fei, "Automatic generation of game levels based on controllable wave function collapse algorithm," in International Conference on Entertainment Computing, Springer 2020, pp. 37-50, doi: https://doi.org/10.1007/978-3-030-65736-9_3.

[34]   S. Alaka and R. Bidarra, "Hierarchical semantic wave function collapse," in Proceedings of the 18th International Conference on the Foundations of Digital Games, 2023, pp. 1-10, doi: https://doi.org/10.1145/3582437.3587209.

[35]   R. Bailly and G. Levieux, "Genetic-wfc: Extending wave function collapse with genetic search," IEEE Transactions on Games, vol. 15, no. 1, pp. 36-45, 2022, doi: https://doi.org/10.1109/TG.2022.3192930.

[36]   K. S. Chicherina, "Application of the wave function collapse algorithm for sample images generation," Informatization and communication, 2021.

[37]   I. Karth and A. M. Smith, "WaveFunctionCollapse is constraint solving in the wild," in Proceedings of the 12th International Conference on the Foundations of Digital Games, 2017, pp. 1-10.

[38]   Q. E. Morris, "Modifying Wave function collapse for more complex use in game generation and design," 2021.

[39]   F. Yiu et al., "A Markovian Framing of WaveFunctionCollapse for Procedurally Generating Aesthetically Complex Environments," arXiv preprint arXiv:2509.09919, 2025.

[40]   M. K. Chung, "Gaussian kernel smoothing," arXiv preprint arXiv:2007.09539, 2020.

[41]   A. Cotter, J. Keshet, and N. Srebro, "Explicit approximations of the Gaussian kernel," arXiv preprint arXiv:1109.4603, 2011.

[42]   S. Smyl, C. Bergmeir, A. Dokumentov, X. Long, E. Wibowo, and D. Schmidt, "Local and global trend Bayesian exponential smoothing models," International Journal of Forecasting, vol. 41, no. 1, pp. 111-127, 2025.

[43]   B. Naima et al., "Enhancing MPPT optimization with hybrid predictive control and adaptive P&O for better efficiency and power quality in PV systems," Scientific reports, vol. 15, no. 1, p. 24559, 2025.